



Data Article

Data of fixed-target pink-beam serial synchrotron crystallography at the Pohang Light Source II

Yongsam Kim^a, Ki Hyun Nam^{b,*}^a Pohang Accelerator Laboratory, Pohang 37673, Republic of Korea^b College of General Education, Kookmin University, Seoul 02707, Republic of Korea

ARTICLE INFO

Article history:

Received 28 November 2023

Revised 14 May 2024

Accepted 4 June 2024

Available online 10 June 2024

Dataset link: [Hit images of lysozyme \(Original data\)](#)Dataset link: [Structure factor and coordinates of glucose isomerase \(Original data\)](#)Dataset link: [Hit images of glucose isomerase \(Original data\)](#)Dataset link: [Structure factor and coordinates of lysozyme \(Original data\)](#)*Keywords:*

Serial synchrotron crystallography

Pink-beam

Fixed-target scan

Glucose isomerase

Lysozyme

ABSTRACT

Pink-beam serial synchrotron crystallography (SSX) is beneficial in terms of X-ray flux and overcoming partial reflection compared with SSX using a monochromatic beam. The fixed-target (FT) scanning method can minimize the physical damage on the crystal sample when delivering the crystals to the X-ray interaction point. Additionally, general researchers can easily access the experiment since no specialized sample transfer technology is needed. The fixed-target pink-beam SSX at the 1C beamline at the Pohang Light Source II (PLS-II) was previously demonstrated using a newly developed magnetic-based sample holder. The room-temperature structure of glucose isomerase and lysozyme were determined using FT pink-beam SSX. Meanwhile, the SSX dataset for glucose isomerase and lysozyme images containing the high X-ray background and multi-crystal hits. These data can be tentatively used to develop an indexing algorithm and practice processing the SX data. This study used detailed information on the diffraction data of fixed-target pink-beam SSX at PLS-II to access the raw data and process the information.

© 2024 The Authors. Published by Elsevier Inc.

This is an open access article under the CC BY-NC license (<http://creativecommons.org/licenses/by-nc/4.0/>)

* Corresponding author.

E-mail address: structure@kookmin.ac.kr (K.H. Nam).

Specifications Table

Subject	Biological sciences
Specific subject area	Structural Biology
Data format	Raw, Analyzed
Type of data	X-ray diffraction data, Table, Image, Graph, Figure
Data collection	Synchrotron: Pohang Light Source II (PLS-II) Beamline: 1C X-ray wavelength: 14820 eV X-ray bandwidth ($\Delta E/E$): 1.2 % Photon flux: $\sim 1 \times 10^{11}$ photons/s Beam size: $130 \times 100 \mu\text{m}$ (full width at half maximum, vertical x horizontal) Sample delivery: fixed-target scanning Sample holder: nylon-mesh and enclosing film (NAM) based sample holder Scan speed: 1.786 mm/s Detector: Pilatus3S 2M (DECTRIS). Data acquisition: 10 Hz Data collection temperature: $24 \pm 0.4 \text{ }^\circ\text{C}$
Data source location	Institution: Kookmin University City/Town/Region: Seoul Country: Republic of Korea
Data accessibility	1. Raw data diffraction images Repository name: ZENODO 1) Data 1: Room-temperature structure of glucose isomerase by fixed-target pink-beam serial synchrotron crystallography - Digital Object Identifier: https://doi.org/10.5281/zenodo.8347473 - Direct URL to data: https://zenodo.org/records/8347473 2) Data 2: Room-temperature structure of lysozyme by fixed-target pink-beam serial synchrotron crystallography - Digital Object Identifier: https://doi.org/10.5281/zenodo.8354296 - Direct URL to data: https://zenodo.org/records/8354296 2. Structure factor and coordinate Repository name: Protein Data Bank (PDB, http://rcsb.org) 1) Data 1: Crystal structure of glucose isomerase by fixed-target pink-beam serial synchrotron crystallography - PDB code: 8WDH - Data identification number: https://doi.org/10.2210/pdb8WDH/pdb - Direct URL to data: https://www.rcsb.org/structure/8WDH 2) Data 2: Crystal structure of lysozyme by fixed-target pink-beam serial synchrotron crystallography - PDB code: 8WDI - Data identification number: https://doi.org/10.2210/pdb8WDI/pdb - Direct URL to data: https://www.rcsb.org/structure/8WDI
Related research article	Y. Kim, K.H. Nam, Fixed-target Pink-Beam Serial Synchrotron Crystallography at Pohang Light Source II, Crystals (2023) [1] https://doi.org/10.3390/cryst13111544

1. Value of the Data

- The first fixed-target pink-beam serial synchrotron crystallography experiment at Pohang Light Source II was demonstrated.
- The crystal structures of glucose isomerase and lysozyme were determined using the FT pink-beam SSX experiment.
- Pink-beam diffraction images with stretch-shaped Bragg peaks can be used to develop an indexing program.
- Diffraction images with the high background scattering generated by the pink beam can be used to develop an indexing program.

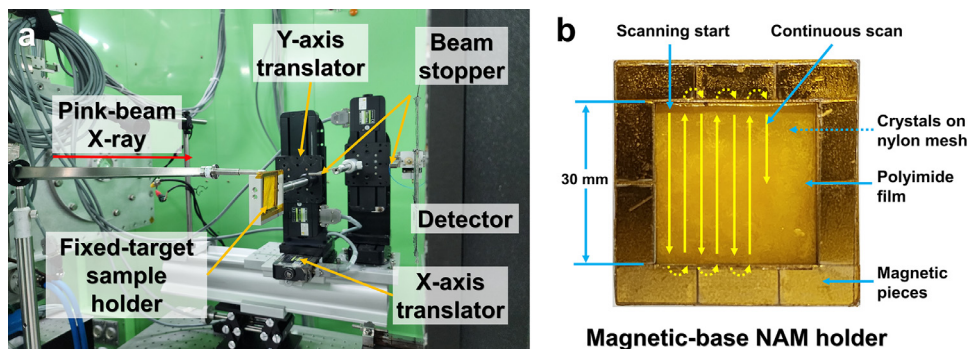


Fig. 1. Fixed-target pink-beam SSX experiment at 1C beamline at PLS-II. (a) Experimental setup for FT pink-beam SSX. (b) Schematic drawing of the fixed-target scanning procedure. Yellow arrows indicate the scanning direction. (For interpretation of the references to color in this figure legend, the reader is referred to the web version of this article.)

2. Background

Serial synchrotron crystallography (SSX) experiments minimize radiation damage and determine the room-temperature structure of macromolecules [1]. Pink-beam SSX technique provides a higher photon flux than monochromatic-beam SSX experiments [2,3]. Accordingly, the diffraction intensity using the pink-beam SSX is higher than that using a monochromatic beam for the same X-ray exposure time. Reducing the exposure time in the high photon flux pink-beam SSX further minimizes potential radiation damage and shortens the data collection time [2]. Furthermore, data collection using a pink-beam SSX can reduce the partial reflection issue of an SSX experiment using a monochromatic beam [2–4]. The fixed-target scanning method helps minimize physical damage to the crystal samples during data collection, and the crystals can be moved to the desired location via programming [5–8]. This method can reduce sample consumption compared with the commonly used injector-based sample delivery method [9].

The fixed-target serial synchrotron crystallography experiment was recently demonstrated at beamline 1C at PLS-II [1]. Some issues with the high background noise generated by the pink beam and multi-crystal hits due to the large beam size and high crystal density were observed during data collection. These issues can be resolved by installing an additional instrument (e.g., specialized capillary) on the beamline and controlling the crystal density on the sample holder. Meanwhile, the high background noise and multi-crystal hit images obtained in this experiment can be used for data processing practice and develop indexing algorithms. For potential uses of the FT pink-beam SSX data, data collection, processing, and access are detailed here.

3. Data Description

Glucose isomerase and lysozyme crystals were used as model samples to demonstrate the FT pink-beam SSX experiment. These crystals were deposited into a newly developed magnetic-based nylon mesh and enclosed film (NAM) sample holder [1]. This sample holder comprises a magnetic frame for enclosing crystal samples; thus, the operation is simpler than the previous method of enclosing the chip using polyimide tape [5–8]. Moreover, dehydration of the crystal solution can be minimized when assembling the sample holder compared with the previous method using polyimide tape. The sample holder containing the crystals was mounted on a translator with a five-phase motor (Fig. 1a). Because of the specifications of the motor used in the translator, when performing a raster scan, the movement time is longer than the data collection time. Accordingly, considering beam time efficiency, SSX data were collected while continuously moving the sample holder rather than raster scanning. The size of the X-ray beam

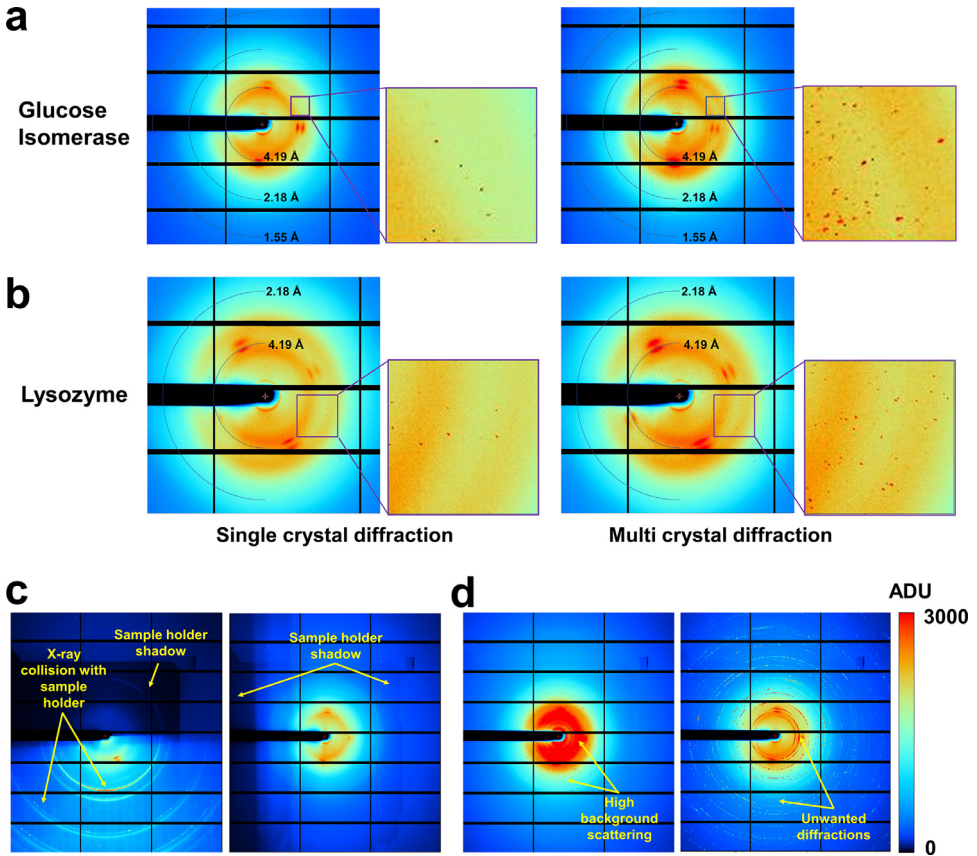


Fig. 2. Collected images from the fixed-target pink-beam SSX experiment. Single-crystal and multi-crystal diffraction patterns from (a) glucose isomerase and (b) lysozyme datasets. (c) Image with unwanted filtered results. (d) Images with high background scattering from the lysozyme dataset.

at the sample holder was approximately $130 \mu\text{m} \times 100 \mu\text{m}$ (vertical \times horizontal, full width at half maximum). The sample holder was continuously moved in the vertical direction and exposed to X-rays during data collection. To avoid exposing the crystal sample to X-rays twice, the sample holder was moved in the horizontal direction at intervals of $400 \mu\text{m}$, considering the beam size (Fig. 1b).

Because of the crystal suspension being deposited in the sample holder, solvent scattering occurs from the crystallization solution and diffraction from the crystals. Additionally, X-rays penetrating the sample holder produce background scattering from the nylon mesh and polyimide film, which are components of the NAM sample holder. Background scattering from water, nylon mesh, and polyimide film was observed at approximately 3.2, 3.4/4.5, and 15 Å, respectively (Fig. 2a and b). Water from the crystallization solution may settle around the crystal sample, between nylon mesh pores or polyimide film, or accumulate by gravity at the bottom of the sample holder. As water thickness differs depending on its location, the background scattering caused by the water also differs from image to image. Water molecules exhibit a typical ring scattering pattern (Fig. 2a and b). The nylon mesh comprises fibers that produce a fiber scattering pattern. Passing through one nylon mesh fiber leads to two symmetrical patterns centered on the beam center. Four scattering patterns are generated when two fibers of the nylon mesh pass through the cross-section. Conversely, the nylon scattering pattern does not appear when

X-rays pass through nylon mesh pores during scanning. Meanwhile, the polyimide film used to prevent dehydration of the crystal suspension maintains an almost constant thickness when exposed to X-rays. Consequently, background scattering of almost similar intensity with an almost identical ring pattern is continuously shown in the collected images. The Bragg peaks of the glucose isomerase and lysozyme crystals exhibited the typical stretched shape observed in typical SSX experiments using the pink-beam [1,2,10].

The glucose isomerase and lysozyme diffraction data included images containing single-crystal and multocrystal diffraction patterns. The occurrence of many multi-crystal hits was due to the high crystal density rather than the large beam used in the experiment. Besides images containing Bragg peaks generated from the crystal samples, the filtered images also included some with very high background scattering or diffraction patterns generated when some of the X-rays collided with the sample holder frame during the sample holder scan (Fig. 2c). Although these images were not used to process data, they can be used as test images in the development of data filtering program algorithms.

During data collection, significantly high X-ray background scattering, which was considered to be an X-ray halo, was detected. This causes the deterioration of data quality. To mitigate background scattering from these X-rays, a slit was used to filter the X-rays except for the main beam. Additionally, another beam stopper was positioned close to the sample. Nevertheless, background scattering remained high at 2000–4000 ADU. This is because the pink-beam exhibits relatively high background scattering compared with the monochromatic beam, and the experiment was conducted without optimizing the beamline instruments owing to the limited beam time. Although the crystal structure was successfully determined in this experiment, higher quality data collection and resolution in structure determination could have been achieved if the high background scattering was minimized. Furthermore, this elevated background scattering diminishes the signal-to-noise ratio (SNR), degrades data quality, and reduces indexing efficiency. Accordingly, these background noises could affect the acquisition of the number of hit images containing Bragg peaks needed for structure determination, as well as indexed patterns that match the input unit cell parameters and crystal system. It was anticipated that these images with high background scattering could be used for data noise filtering processing and indexing practice for researchers generally.

For glucose isomerase, a total of 20,210 images were collected, and 13,592 hit images were obtained. Indexing resulted in a crystal diffraction pattern count of 17,600, approximately 1.3 times higher than the hit image count, indicating a high multi-crystal hit rate. For lysozyme, a total of 18,959 images were collected, and 9,535 hit images were obtained. Indexing led to a crystal diffraction pattern count of 3485. The lower indexing rate for lysozyme is attributed to the weak diffraction intensity of the crystals and insufficient peak separation due to the multi-crystal diffraction patterns.

As shown above, the hit image includes unwanted scattering (Fig. 2c); thus, the hit image count does not solely represent diffraction data containing only Bragg peaks. Additionally, the indexing rate can vary depending on different indexing parameters [11], making the image used to determine the crystal structure in the experiment just a reference number. Furthermore, the values of the indexed image may change depending on the data processing algorithm [12] and optimization of the detector geometry. The information regarding the optimized detector geometry obtained using geoptimiser while processing glucose isomerase and lysozyme data with CrystFEL is presented in Table 1 (Fig. 3).

Glucose isomerase and lysozyme datasets were processed up to 1.7 and 2.2 Å, respectively. Overall completeness, SNR, CC, CC*, and R_{split} values of glucose isomerase were 100, 4.67, 0.8240, 0.9505, and 25.98, respectively (Table 2). Overall completeness, SNR, CC, CC*, and R_{split} values of lysozyme were 100, 5.43, 0.8741, 0.9658, and 5.43, respectively (Table 2). All data collection statistics for glucose isomerase and lysozyme were reasonable for determining the crystal structure, but the CC values were significantly low compared with those of other parameters (Fig. 4). Low CC values indicate poor data quality or insufficient diffraction data volume. This can be improved by collecting more images or lowering the background scatter and multi-crystal hit rate.

Table 1

Detector geometry information.

Detector geometry parameters	Glucose isomerase	Lysozyme
photon_energy	14,815	14,815
Clen	147	147
0/min_fs	0	0
0/max_fs	1474	1474
0/min_ss	0	0
0/max_ss	1678	1678
0/corner_x	−662.418	−662.278
0/corner_y	−867.435	−867.497
0/fs	+0.999999x +0.001766y	+0.999999x +0.001672y
0/ss	−0.001766x +0.999999y	−0.001672x +0.999999y
rigid_group_q0	0	0
rigid_group_a0	0	0
rigid_group_collection_quadrants	q0	q0
rigid_group_collection_asics	a0	a0
0/coffset	0.002034	0.001899

Table 2

Data collection statistics. Processing statistics have been presented elsewhere [1].

Data collection	Glucose isomerase	Lysozyme
X-ray Source	1C, PLS-II	1C, PLS-II
X-ray energy (eV)	14820	14820
X-ray exposure (ms)	100	100
Collected images	20,210	18,959
Hit images	13,592	9535
Indexed patterns	17,626	3485
Space group	I222	P4 ₃ 2 ₁ 2
Cell dimension (Å) a, b, c	94.14, 99.94, 103.16	78.83, 78.83, 38.20
Resolution (Å)	20.00–1.70 (1.76–1.70)	20.00–2.20 (2.27–2.20)
Unique reflections	53,508 (5307)	6509 (628)
Completeness (%)	100.0 (100.0)	100.0 (100.0)
Redundancy	191.5 (256.9)	488.7 (398.5)
SNR	4.67 (4.39)	5.43 (3.74)
CC	0.8239 (0.3692)	0.8737 (0.5245)
CC*	0.9505 (0.7343)	0.9657 (0.8295)
Rsplit (%) ^a	25.98 (27.16)	21.21 (33.46)
Wilson B factor (Å ²)	11.97	23.92

Values for the outer shell are given in parentheses.

^a $R_{split} = (1/\sqrt{2}) \cdot \frac{\sum_{hkl} \left| \frac{F_{obs}^{hkl} - F_{calc}^{hkl}}{F_{obs}^{hkl}} \right|}{\frac{1}{2} \left(\frac{F_{obs}^{hkl} + F_{calc}^{hkl}}{F_{obs}^{hkl}} \right)}$, ^b $R_{work} = \frac{\sum ||F_{obs}^{hkl}| - |F_{calc}^{hkl}||}{\sum |F_{obs}^{hkl}|}$, where F_{obs} and F_{calc} are the observed and calculated structure-factor amplitudes respectively.

The room-temperature structures of glucose isomerase and lysozyme were determined at resolutions of 1.7 Å and 2.2 Å, respectively (Table 3). During refinement, the low-resolution area (beam stopper ~7 Å) with high background scattering was excluded to obtain better R-values. The R_{work}/R_{free} values of glucose isomerase and lysozyme structures were 25.10/27.79 and 25.12/29.93, respectively. The electron density maps of glucose isomerase and lysozyme were clearly observed (Fig. 5). Glucose isomerase contains two metal-binding sites at the active site for the substrate-binding and catalytic reaction [10]. The metal binding geometry of GI is similar to that in a previous report, but different conformations of the His220 residue were observed. The amino acid positions of lysozyme are similar to those in a previous report.

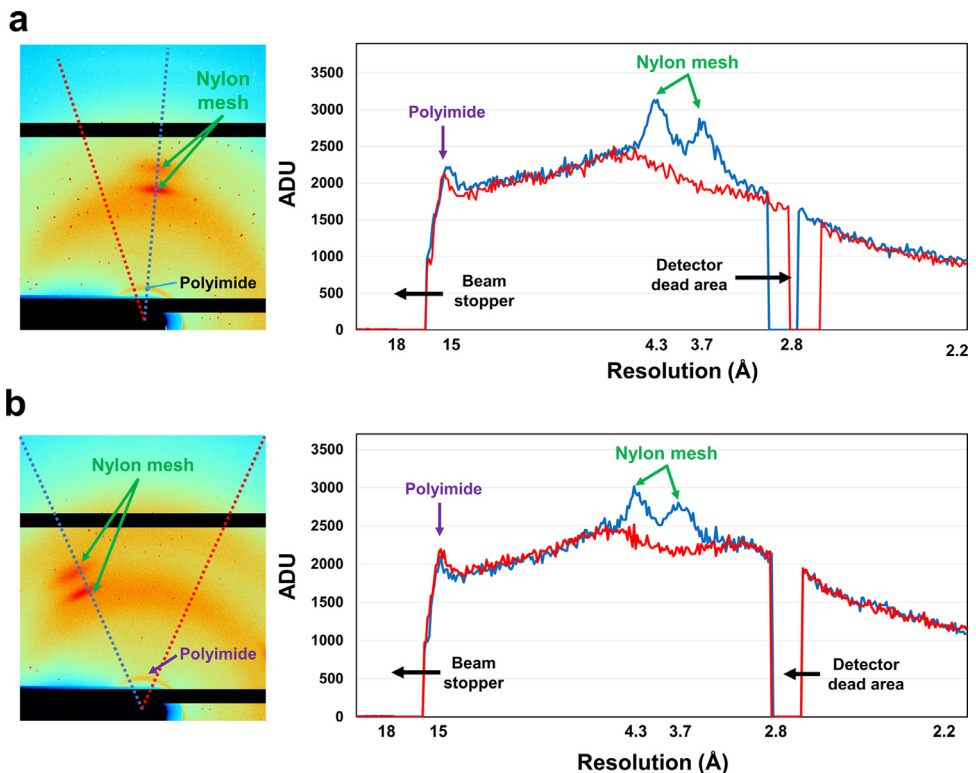


Fig. 3. Analysis of X-ray background noise in the collected images. Close-up image and profile of background noise obtained from (a) glucose isomerase and (b) lysozyme. The profile was obtained from the beam stopper to 2.2 Å resolution. Blue and red lines in the profile are indicated in dot-line in the left image. (For interpretation of the references to color in this figure legend, the reader is referred to the web version of this article.)

4. Experimental Design, Materials and Methods

Protein crystallization, manufacture of magnetic-based sample holder, data collection, and structure determination have been reported [1]. Crystal suspensions of glucose isomerase ($< 5\text{--}300\ \mu\text{m}$) or lysozyme ($\sim 20 \times 20 \times 20\ \mu\text{m}^3$) were deposited on a nylon mesh (pore size: $70\ \mu\text{m}$) in a magnetic-based sample holder. FT pink-beam SSX experiments were performed at beam-line 1C at the Pohang Light Source II (PLS-II, Pohang, Republic of Korea). The pink-beam (energy bandwidth: 1.2% ($\Delta E/E$)) was obtained using the Mo/B₄C multilayer mirror system. The X-ray energy and photon flux were 14820 eV and $\sim 1 \times 10^{11}$ photons/s, respectively. The X-ray sizes were $130 \times 100\ \mu\text{m}$ (vertical \times horizontal, full width at half maximum) at the sample position. A sample holder containing the protein crystals was scanned from the top left to the bottom, then moved to the right at $400\ \mu\text{m}$ and scanned from the bottom to the top. Consequently, the entire sample holder, including the crystal, was scanned in the vertical direction while moving in the horizontal direction. The translation speed in the vertical and horizontal directions was approximately 1.786 mm/sec. The diffraction data were recorded using a Pilatus3S 2M detector (Dectris, Switzerland) at an ambient temperature ($24 \pm 0.4\ ^\circ\text{C}$) with a 10-Hz readout. Hit images containing Bragg peaks were filtered using the Cheetah program [13]. The filter parameters are as follows: cutoff signal/noise = 5, max/min number of connected pixels = 20/2, threshold = 1000, and max/min number of peaks = 5000/30. Diffraction images were indexed, integrated, and scaled using CrystFEL v0.9.1 [14] with XGANDALF [15] or MOSFLM [16] indexing algorithms. The

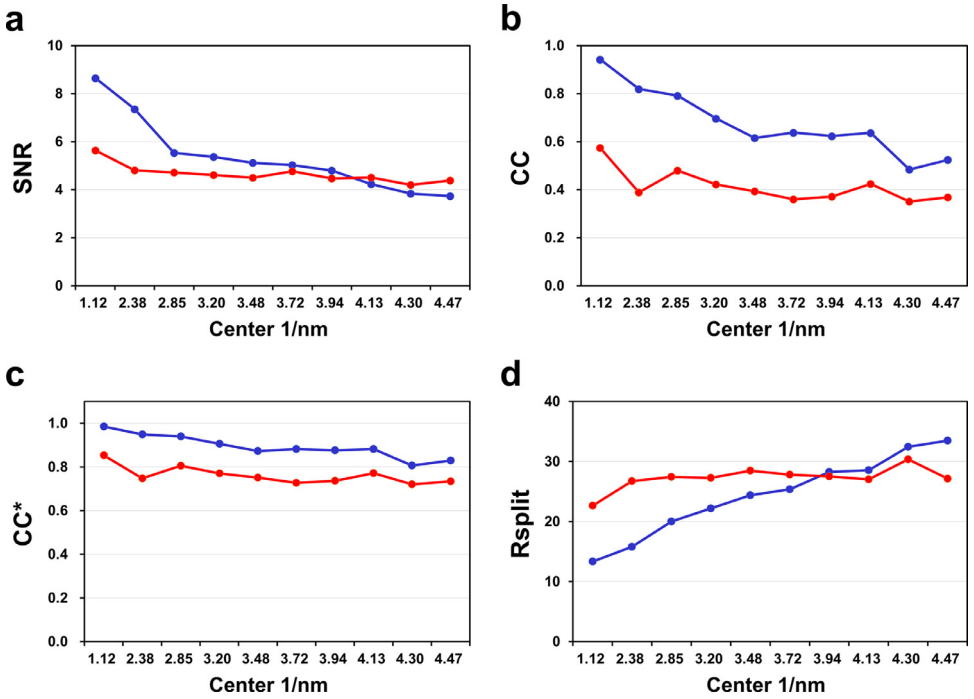


Fig. 4. Data processing profiles of glucose isomerase (red) and lysozyme (blue) for (a) signal-to-noise ratio (SNR), (b) CC, (c) CC*, and (d) Rsplit. (For interpretation of the references to color in this figure legend, the reader is referred to the web version of this article.)

Table 3

Structure refinement statistics. Refinement statistics have been presented elsewhere [1].

Refinement		
Resolution (Å)	7.0–1.70	7.0–1.70
$R_{\text{work}}/R_{\text{free}}^{\text{b}}$	0.2510/0.2779	0.2512/0.2993
R.m.s. deviations		
Bonds (Å)	0.004	0.008
Angles (°)	0.861	0.969
B factors (Å ²)		
Protein	13.42	12.11
Water	7.58	16.24
Ramachandran plot		
Favored (%)	93.46	95.28
Allowed (%)	5.76	4.72
Disallowed	0.79	0.00

R_{free} was calculated as R_{work} using a randomly selected subset of unique reflections not used for structure refinement.

detector geometry was refined using a geoptimiser [17] during indexing. The phasing problem was solved using the molecular replacement method with MOLREP [18]. The crystal structures of glucose isomerase (7CJO) [19] and lysozyme (PDB code 6IG6) [20] were used as search models. The model was built using the COOT [21] program. The structure was refined using phenix.refine in the PHENIX program. Raw data for hit images have been deposited (<http://zenodo.org>). The structural factors and coordinates have been deposited (<http://rcsb.org>).

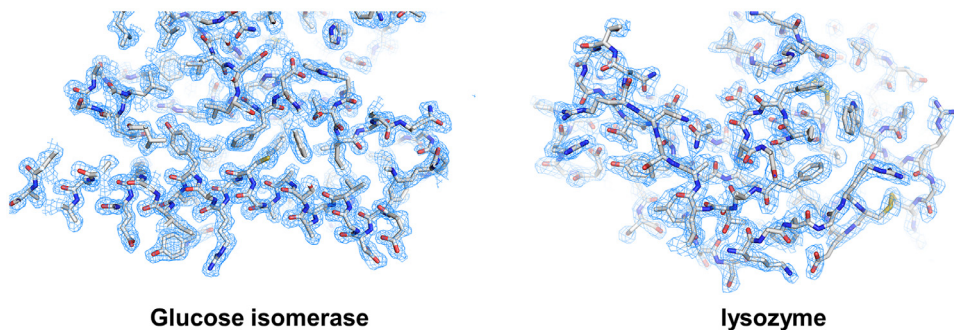


Fig. 5. 2mFo-DFc (sky mesh, 1σ) electron density map of glucose isomerase and lysozyme obtained using fixed-target pink-beam SSX. (For interpretation of the references to color in this figure legend, the reader is referred to the web version of this article.)

Limitations

Data collection for the FT pink-beam SSX experiment was not conducted under optimal beamline conditions. This experiment aimed to demonstrate the FT pink-beam SSX setup, which incorporates a novel sample holder and a continuous scanning method using a large beam.

Ethics Statement

This work meets the ethical requirements for publication in this journal. This work does not involve human subjects, animal experiments, or any data collected from social media.

Data Availability

[Hit images of lysozyme \(Original data\)](#) (Zenodo)

[Structure factor and coordinates of glucose isomerase \(Original data\)](#) (PDB)

[Hit images of glucose isomerase \(Original data\)](#) (Zenodo)

[Structure factor and coordinates of lysozyme \(Original data\)](#) (PDB)

CRediT Author Statement

Yongsam Kim: Data curation, Writing – review & editing; **Ki Hyun Nam:** Data curation, Formal analysis, Validation, Visualization, Writing – original draft, Funding acquisition.

Acknowledgments

The author acknowledges support at beamline 1C, Pohang Accelerator Laboratory, Pohang, South Korea. Experiments at the 1C beamline, PLS-II, were supported by MSIT. The authors also thank the Global Science experimental Data hub Center (GSDC) at the Korea Institute of Science and Technology Information (KISTI) for providing computing resources and technical support. This work was funded by the National Research Foundation of Korea (NRF) (NRF-2017M3A9F6029736 and NRF-2021R111A1A01050838 to K.H.N.), and the Korea Initiative for Fostering University of Research and Innovation (KIURI) Program of the NRF (NRF-2020M3H1A1075314 to K.H.N.). This study was supported by ProGen (to K.H.N.).

Declaration of Competing Interest

The authors declare that they have no known competing financial interests or personal relationships that could have appeared to influence the work reported in this paper.

References

- [1] Y. Kim, K.H. Nam, Fixed-target pink-beam serial synchrotron crystallography at Pohang Light Source II, *Crystals* 13 (11) (2023) 1544, doi:[10.3390/cryst13111544](https://doi.org/10.3390/cryst13111544).
- [2] A. Meents, M.O. Wiedorn, V. Srajer, R. Henning, I. Sarrou, J. Bergtholdt, M. Barthelmess, P.Y.A. Reinke, D. Dierksmeyer, A. Tolstikova, S. Schaible, M. Messerschmidt, C.M. Ogata, D.J. Kissick, M.H. Taft, D.J. Manstein, J. Lieske, D. Oberthuer, R.F. Fischetti, H.N. Chapman, Pink-beam serial crystallography, *Nat. Commun.* 8 (1) (2017) 1281, doi:[10.1038/s41467-017-01417-3](https://doi.org/10.1038/s41467-017-01417-3).
- [3] J.M. Martin-Garcia, L. Zhu, D. Mendez, M.-Y. Lee, E. Chun, C. Li, H. Hu, G. Subramanian, D. Kissick, C. Ogata, R. Henning, A. Ishchenko, Z. Dobson, S. Zhang, U. Weierstall, J.C.H. Spence, P. Fromme, N.A. Zatsepin, R.F. Fischetti, V. Cherezov, W. Liu, High-viscosity injector-based pink-beam serial crystallography of microcrystals at a synchrotron radiation source, *IUCrj* 6 (3) (2019) 412–425, doi:[10.1107/s205225251900263x](https://doi.org/10.1107/s205225251900263x).
- [4] C. Dejoie, L.B. McCusker, C. Baerlocher, R. Abela, B.D. Patterson, M. Kunz, N. Tamura, Using a non-monochromatic microbeam for serial snapshot crystallography, *J. Appl. Crystallogr.* 46 (3) (2013) 791–794, doi:[10.1107/s0021889813005888](https://doi.org/10.1107/s0021889813005888).
- [5] D. Lee, S. Baek, J. Park, K. Lee, J. Kim, S.J. Lee, W.K. Chung, J.L. Lee, Y. Cho, K.H. Nam, Nylon mesh-based sample holder for fixed-target serial femtosecond crystallography, *Sci. Rep.* 9 (1) (2019) 6971, doi:[10.1038/s41598-019-43485-z](https://doi.org/10.1038/s41598-019-43485-z).
- [6] K. Lee, D. Lee, S. Baek, J. Park, S.J. Lee, S. Park, W.K. Chung, J.L. Lee, H.S. Cho, Y. Cho, K.H. Nam, Viscous-medium-based crystal support in a sample holder for fixed-target serial femtosecond crystallography, *J. Appl. Crystallogr.* 53 (4) (2020) 1051–1059, doi:[10.1107/S1600576720008663](https://doi.org/10.1107/S1600576720008663).
- [7] S.Y. Park, H. Choi, C. Eo, Y. Cho, K.H. Nam, Fixed-target serial synchrotron crystallography using nylon mesh and enclosed film-based sample holder, *Crystals* 10 (9) (2020) 803, doi:[10.3390/cryst10090803](https://doi.org/10.3390/cryst10090803).
- [8] K.H. Nam, J. Kim, Y. Cho, Polyimide mesh-based sample holder with irregular crystal mounting holes for fixed-target serial crystallography, *Sci. Rep.* 11 (1) (2021) 13115, doi:[10.1038/s41598-021-92687-x](https://doi.org/10.1038/s41598-021-92687-x).
- [9] J. Park, K.H. Nam, Sample delivery systems for serial femtosecond crystallography at the PAL-XFEL, *Photonics* 10 (5) (2023), doi:[10.3390/photonics10050557](https://doi.org/10.3390/photonics10050557).
- [10] Y. Kim, K.H. Nam, Pink-beam serial synchrotron crystallography at Pohang Light Source II, *Crystals* 12 (11) (2022) 1637, doi:[10.3390/cryst12111637](https://doi.org/10.3390/cryst12111637).
- [11] K.H. Nam, Hit and indexing rate in serial crystallography: incomparable statistics, *Front. Mol. Biosci.* 9 (2022) 858815, doi:[10.3389/fmolb.2022.858815](https://doi.org/10.3389/fmolb.2022.858815).
- [12] K.H. Nam, Processing of multicrystal diffraction patterns in macromolecular crystallography using serial crystallography programs, *Crystals* 12 (1) (2022) 103, doi:[10.3390/cryst12010103](https://doi.org/10.3390/cryst12010103).
- [13] A. Barty, R.A. Kirian, F.R. Maia, M. Hantke, C.H. Yoon, T.A. White, H. Chapman, Cheetah: software for high-throughput reduction and analysis of serial femtosecond X-ray diffraction data, *J. Appl. Crystallogr.* 47 (3) (2014) 1118–1131, doi:[10.1107/S1600576714007626](https://doi.org/10.1107/S1600576714007626).
- [14] T.A. White, V. Mariani, W. Brehm, O. Yefanov, A. Barty, K.R. Beyerlein, F. Chervinskii, L. Galli, C. Gati, T. Nakane, A. Tolstikova, K. Yamashita, C.H. Yoon, K. Diederichs, H.N. Chapman, Recent developments in CrystFEL, *J. Appl. Crystallogr.* 49 (2) (2016) 680–689, doi:[10.1107/S16005767160004751](https://doi.org/10.1107/S16005767160004751).
- [15] Y. Gevorkov, O. Yefanov, A. Barty, T.A. White, V. Mariani, W. Brehm, A. Tolstikova, R.R. Grigat, H.N. Chapman, XGAN-DALF - extended gradient descent algorithm for lattice finding, *Acta Crystallogr. A Found. Adv.* 75 (5) (2019) 694–704, doi:[10.1107/S2053273319010593](https://doi.org/10.1107/S2053273319010593).
- [16] T.G. Battye, L. Kontogiannis, O. Johnson, H.R. Powell, A.G. Leslie, iMOSFLM: a new graphical interface for diffraction-image processing with MOSFLM, *Acta Crystallogr. D Biol. Crystallogr.* 67 (4) (2011) 271–281, doi:[10.1107/S0907444910048675](https://doi.org/10.1107/S0907444910048675).
- [17] O. Yefanov, V. Mariani, C. Gati, T.A. White, H.N. Chapman, A. Barty, Accurate determination of segmented X-ray detector geometry, *Opt. Express* 23 (22) (2015) 28459–28470, doi:[10.1364/OE.23.028459](https://doi.org/10.1364/OE.23.028459).
- [18] A. Vagin, A. Teplyakov, Molecular replacement with MOLREP, *Acta Crystallogr. D Biol. Crystallogr.* 66 (1) (2010) 22–25, doi:[10.1107/S0907444909042589](https://doi.org/10.1107/S0907444909042589).
- [19] K.H. Nam, Crystal structure of the metal-free state of glucose isomerase reveals its minimal open configuration for metal binding, *Biochem. Biophys. Res. Commun.* 547 (2021) 69–74, doi:[10.1016/j.bbrc.2021.02.026](https://doi.org/10.1016/j.bbrc.2021.02.026).
- [20] J. Park, S. Park, J. Kim, G. Park, Y. Cho, K.H. Nam, Polyacrylamide injection matrix for serial femtosecond crystallography, *Sci. Rep.* 9 (1) (2019) 2525, doi:[10.1038/s41598-019-39020-9](https://doi.org/10.1038/s41598-019-39020-9).
- [21] P. Emsley, K. Cowtan, Coot: model-building tools for molecular graphics, *Acta Crystallogr. D Biol. Crystallogr.* D60 (2004) 2126–2132, doi:[10.1107/S0907444904019158](https://doi.org/10.1107/S0907444904019158).